Final Report
Award ID 0710937 / G10AP00023
Contemporary Strain and Stressing Rates in Central and Southern Alaska Through the Earthquake Cycle

Executive Summary

The subduction of the Pacific Plate beneath North America induces broad scale stressing of the Alaskan crust that has led to the development of the highest mountains in North America, the highest slip rates along some of the longest strike-slip faults on Earth, and widespread seismicity that includes the 1964 M9.2 Alaska earthquake, the second largest ever recorded. These features are a consequence of deformation associated with three primary processes, interseismic loading due to relative plate motions, large earthquakes, and postseismic processes. How these mechanisms contribute to the evolution of stress in the Alaskan crust is not well understood. This project sought to understand the relative contributions of these processes to the contemporary velocity field in central and southern Alaska, then use this knowledge to calculate interseismic stressing rates as well as the evolution of stress due to coseismic slip and postseismic processes associated with the 1964 Alaska quake and the last three major earthquakes on the Fairweather and Queen-Charlotte faults. The approach was to develop finite element models that could consider complex factors including the geometry of the Pacific/North American interface, which varies from shallow to deeply slipping along a strike that curves significantly, the locking depth of the megathrust, and the rheology of the lower crust and upper mantle.

Results suggest that interseismic deformation and on-going postseismic deformation following the 1964 earthquake both contribute significantly to the GPS measured contemporary velocity field. Viscoelastic relaxation associated with a mantle with a viscosity of ~10^{19} Pa s is required to explain southerly directed velocities that are observed in the Cook Inlet region to well north of the Denali fault. Results also suggest that subduction of the Pacific plate leads to a broad zone of deformation with high stressing rates concentrated in a band that lies several hundred kilometers from the plate boundary, coeval with the inboard location of the maximum locking depth of the megathrust. Interseismic deformation and stressing rates remain high further inland across the Yakutat microplate, where flat subduction extends the width of the locked plate interface. Calculations show that postseismic relaxation following the large strike slip events serves to reload these rupture surfaces while relieving stress on the eastern Denali Fault. Postseismic relaxation following the 1964 earthquake combined with coseismic stress changes, promoted the triggering of the 2002 Denali quake. Calculations also suggest that over the past 50 years high stress has accumulated on part of the thrust interface to the west and east of the 1964 rupture surface and along the Queen-Charlotte Fault to the south of the 1949 rupture surface.

In addition to earthquake triggering, our research also sought to understand whether or not their exists a Fairweather-Totschunda connecting fault between the Denali-Totschunda fault system and that of the Fairweather Fault. This region is at high elevation and under numerous glaciers, making it difficult to determine whether an active fault exists in this region. We developed a shells finite element model that where known slip rates where applied to known active faults, then solved for the long-term slip rate on a potential Fairweather-Totschunda fault, testing each model against the contemporary GPS velocity field. Results suggest that a

Fairweather-Totschunda fault exists with a long-term slip rate of the order of 8 mm/yr, suggesting that it is a heretofore-seismic hazard that should probably be considered in seismic hazard maps of Alaska.

A paper covering the details postseismic study can by found in: Ali, S. T. and A. M. Freed, Contemporary deformation and stressing rates in Southern Alaska, Geophys. J. Inter, *183,* 557-571, 2010. A paper on the proposed Fairweather-Totschunda Fault is forthcoming.

1. Introduction

Few regions on Earth show the large-scale consequences of subduction as well as those observed in central and southern Alaska (Figure 1). This area is characterized by rapid uplift of the Alaska, Wrangell, and St. Elias mountain ranges, the highest in North America; high slip rates (up to 50 mm/year) along some of the largest (>1000 km) strike-slip faults on Earth, such as the long Queen Charlotte-Fairweather and Denali fault system; and most importantly from a hazard standpoint, widespread seismicity, including the 1964 M9.2 Alaska quake, the second largest earthquake ever recorded [Kanamori, 1977], and the 2002 M7.9 Denali earthquake, the largest earthquake to occur within the North American continent in the past century [Eberhart-Phillips et al., 2003].

The timing and spatial extent of large earthquakes is a function of the evolution of stress in the upper crust. Knowledge of stressing rates is a powerful tool for assessing seismic hazards, as it cannot only be used to understand past events, but also to predict where future earthquakes are likely to occur. Contemporary stressing rates can be constrained (in part) by observations of surface velocities (Figure 2). Comprehensive GPS observations made between 1997-2002 [Freymueller et al., 2008] have illuminated the contemporary velocity field of Southern Alaska prior to disruption of this field by the 2002 M7.9 Denali earthquake [Eberhart-Phillips, 2003; Freed et al., 2006a]. Most of the observed velocities in the region trend northwestwards, coinciding with the general direction of the Pacific plate convergence. However, a number of stations in the Cook Inlet area (just north of the vicinity of the 1964 rupture surface), as well as further inland near Fairbanks and beyond, show velocity vectors that trend southeastwards. These velocities have generally been attributed to on-going transient processes associated with 1964 Alaska quake, including postseismic relaxation and afterslip or a combination of both [Cohen and Freymueller, 2004; Zweck et al., 2002; Suito and Freymueller, 2009].

Here we sought to understand the relative contributions of interseismic and postseismic processes to the contemporary velocity field in central and southern Alaska, then use this knowledge to calculate interseismic stressing rates as well as the evolution of stress due to coseismic slip and postseismic processes associated with the 1964 Alaska quake and the last three major earthquakes on the Fairweather and Queen-Charlotte faults. These processes are influenced by a wide variety of factors including the geometry of the Pacific/North American interface, which varies from shallow to deeply slipping along a strike that curves significantly (Figure 1), the locking depth of the megathrust, and the rheology of the lower crust and upper mantle. To this end we developed a numerical viscoelastic model that could consider these complexities and used it to determine the set of interseismic and postseismic parameters required to explain the contemporary surface velocity field. Our stress evolution calculations concentrated on questions such as the magnitude and orientation of stresses transferred inland from the plate boundary to drive motion on the Denali Fault and how the evolution of transient stresses may have influenced the 2002 Denali earthquake.

2. Analysis Approach

Our analysis utilized several numerical models, one that considered the full 3-D geometry and mechanical behavior of the Pacific-Alaskan margin, and two 2-D models that cut across the Yakutat microplate and across the 1964 rupture surface (Figure 3). The 2-D models enabled us to explore interseismic and postseismic modeling approaches and parameter space in an efficient manner, enabling a more narrow focus with the computationally expensive 3-D calculations. The north, west, and eastern model boundaries of these are held fixed. For runs that consider the motion of the subducting Pacific plate over time, a velocity boundary condition was applied to the two ends of the slab, consistent with the motion of the Pacific plate relative to North America in accordance with NUVEL-1A [DeMets et al., 1994]. This velocity varies from ~48 mm/yr at the eastern edge of the Yakutat microplate to ~65 mm/yr at the western edge of the model domain. The geometry and extent of the slab was based on published slab contours and observed seismicity [Eberhart-Phillips, 2006]. The oceanic lithosphere is assumed to be 80 km thick and behaves elastically in all runs. An average thickness of 37.5 km for the continental crust is assumed, based on tomographic data of Eberhart-Phillips [2006] and receiver function analysis of Veenstra et. al [2006]. The geometry and slip distribution for earthquakes was based on Nishenko and Jacob [1990] and Johnson et al. [1996].

We assumed a linear Newtonian viscoelastic rheology, which enables us to calculate separately and superimpose interseismic and postseismic results. The viscosity structure of the lower crust and mantle wedge has been inferred from GPS observations of postseismic relaxation following the 2002 Denali earthquake. The most appropriate study would be the power-law study of Freed et al. [2006b], as it estimates the magnitude of the longer-term (interseismic) viscosity structure of the lower crust and mantle wedge after the non-linear portion of a transient phase has diminished. This study suggested a mantle viscosity below 80 km of order $1\text{-}3\times10^{19}$ Pa s and a mantle viscosity above 80 km depth of order $3\text{-}5\times10^{19}$ Pa s, and a moderately stronger (10^{20} Pa s) lower crust.

Interseismic deformation rates have been numerically simulated using a number of different approaches. The key was to find an interseismic process that explains why high interseismic strain rates are concentrates just inboard of the subduction interface. We utilized a modified backslip model [Zhao and Takemoto, 2000], in which slip is imposed below the locked portion of the interface, and at the base of the down-going slab; a spin-up model where interseismic surface velocities are modeled as the cumulative effect of postseismic relaxation following a number of previous earthquake cycles [e.g., Hetland and Hager, 2006]; and by consideration of a lateral zone of weak upper crust that accommodates more strain then surrounding regions. Our analysis approach was to initially explore the various methods for simulating interseismic deformation in southern Alaska using the 2-D model to guide us toward the best approach to use with the 3-D model. For brevity of this report, we will not discuss the 2-D interseismic results except to state that the modified back slip model provided the best solution in terms of computational efficiency and reasonableness of results and was thus used for our 3-D study. We similarly use the 2-D model to explore parameter space associated with postseismic relaxation and afterslip processes to guide us toward the models that are going to likely work best in 3-D. We found that a model in which the lower crust and upper mantle has an average viscosity of 1.5×10^{19} Pa s provides a good overall fit through the two cross-sections considered. The observed velocities can also be explained by a viscosity structure where the lower crust has a viscosity three times that of the upper mantle (3×10^{19} compared to 1×10^{19} Pa s). Such a model would be more consistent with a

decrease in viscosity with depth found in several postseismic studies following the 2002 Denali earthquake [Pollitz et al., 2005, Freed et al., 2006a]. 2-D calculations were accomplished using GeoFEST [Parker, 2008], while 3-D calculations used PyLith [Aagaard et al., 2008, 2009].

3. Results

Guided by the 2-D modeling results, we used the 3-D model to understand the broad response of the Alaskan lithosphere to coseismic, postseismic, and interseismic processes. For the interseismic model we use the modified backslip approach assuming a locking depth of 15 km along the strike slip faults, and 30 km along the megathrust. Model results show a good fit to GPS observations in regions not significantly influenced by postseismic processes (Figure 4a). The interseismic only model explained well the GPS observations of higher velocities near the Yakutat coast and on Kodiak Island and west of this region. It also matched the counter-clockwise rotation of the velocity field just south of the Denali Fault, an indication of how subduction of the Pacific Plate drives inland shear taken up by this fault.

The interseismic model could not explain southwardly directed velocities near the Cook Inlet region and north of the Denali Fault. Nor could this model explain northwest trending velocities to the east of the Fairweather and Queen-Charlotte Faults. These deficiencies are more easily observed by plotting the interseismic residuals i.e., GPS observed minus calculated interseismic velocities (black arrows in Figure 4b). The systematic pattern of trenchward directed residual velocities near the rupture zone of the 1964 Great Alaska earthquake is strongly suggestive of a postseismic process. Likewise for small southeastwardly directed residual velocities just east of the Fairweather and Queen-Charlotte Faults considering the proximity of the 1949, 1958 and 1972 events.

To study the influence of postseismic relaxation following these four historic earthquakes, we simulated the slip of each event in a time consistent fashion and calculated predicted surface velocities in the year 2001. The calculated postseismic relaxation velocities associated with a model that assumes a lower crustal viscosity of $3x10^{19}$ Pa s and a mantle viscosity of $1x10^{19}$ Pa s provided a good fit to interseismic residual velocities (Figure 4b). In general, the interseismic residuals are well explained by viscoelastic relaxation, especially in the region north of the Cook Inlet as well as inland north of the Denali Fault. The relaxation model poorly fits the interseismic residuals near the north and western edges of the Kenai Peninsula (Figure 4b), as magnitude of the modeled velocities is significantly smaller than the residuals.

The region between Kodiak Island and the Kenai Peninsula happens to correspond to a region that accommodated minimal slip between slip patches in a two-patch model suggested by Johnson et al. [1996]. This region, shown as a hachured area within the 1964 rupture surface in Figure 4c, may be responding to coseismic stress changes associated with slip on the neighboring patches. If we assume that this region is currently slipping at about the rate of Pacific plate convergence and add the resulting afterslip surface velocities to that of the viscoelastic relaxation model, we find that the combined velocities provides an improved fit to the interseismic residual velocities (Figure 4c) as the magnitudes are now correctly estimated.

Interpretation of interseismic residual velocities near the Fairweather and Queen-Charlotte Faults was more difficult to understand. Southerly-directed residual velocities in this region are explained by viscoelastic relaxation (Figure 4b). But there are a number of residual velocities, most notably east of the Fairweather fault, which are directed to the northeast. There was no aspect of an interseismic, viscoelastic relaxation, or afterslip calculation that could explain such

velocity vectors. However, this region is currently being influenced by the world's fastest present day glacial unloading, which has been ongoing since the Little Ice Age (LIA) terminated around 1800-1850 [e.g., Sauber et al., 2000]. LIA retreat is currently inducing more than 30 mm/yr of uplift centered in the Glacier Bay region (on the coast at ~59N) [Larsen et al., 2004, 2005]. The horizontal velocities associated with this process have not yet been determined, but one would expect a pattern in which these velocities would radiate out from the area, consistent with the northeastern directed velocities observed to the west. More work needs to be accomplished in this region once a postglacial horizontal velocity component is established.

Calculated contemporary velocities based on a combined interseismic, viscoelastic relaxation, and afterslip model are compared to those observed by GPS in Figure 2. Overall there was good agreement between the observed and calculated velocity fields. Our results for the region surrounding the 1964 rupture zone are also in general agreement with that of Suito and Freymueller [2009]. This demonstrates that, to a first order, contemporary surface velocities in Alaska can be explained as resulting from convergence of the Pacific plate and transient postseismic processes associated with recent (past 50 years) earthquakes in the region.

4. Stress Evolution Calculations

From the 3-D model that explains the contemporary velocity field, we calculated the evolution of stress over the past half-century. We first consider how stressing rates in the Alaskan upper crust are influenced by the relative motion of the Pacific and North American plates. We then consider how stress has evolved on the major active fault systems due to interseismic, coseismic, and postseismic deformation.

Figure 5 shows the calculated maximum compressive and maximum shear stressing rates in the upper North American crust associated with interseismic deformation. Inboard of the subduction zone, rates are greatest in a band located about ~150 km from the plate boundary in the southwest, but about double that distance within the region of the Yakutat microplate. This is consistent with the location where GPS observed velocities were shown to experience a rapid drop-off. This zone of highest compressive and shear stressing rates lies directly above the location of the maximum locking depth, which extends further inland near Yakutat because of shallow subduction (Figure 5). Maximum compressive normal stresses decrease to the south of this region (i.e. over the locked megathrust), as this region represents a zone in which stresses transition from the Pacific plate (low stress due to slab pull) to the North American plate (high stress due to convergence).

The zone of high shear stresses inboard of the subduction zone transitions to an even higher shear stress along the transform portion of the plate boundary (the Fairweather and Queen-Charlotte Fault system), where plate motion is directly associated with shear (Figure 5b). The narrowness of the transform shear zone is consistent with the quickly diminishing magnitude of northwest trending observed velocities eastward from this fault system. Compressional stresses along this boundary (Figure 5a) are a result of a modest azimuth difference between the strike of the Fairweather and Queen-Charlotte faults and the direction of the Pacific Plate relative to North America.

To understand how active faults are influenced by stresses through the earthquake cycle, we calculated changes in Coulomb stress. Coulomb stress calculations quantify how shear and normal stress changes act to push faults closer to (positive Coulomb stress change) or further

away from (negative Coulomb stress change) failure [e.g., Jaeger and Cook, 1979; Stein and Lisowski, 1983; King et al., 1994; Freed, 2005]. Here we calculate the change in Coulomb stress,

$$\Delta\sigma_c = \Delta\tau - \mu' \Delta\sigma_n$$

where $\Delta\tau$ is the change in shear stress parallel to the slip direction of a fault, $\Delta\sigma_n$ is change in fault-normal (or clamping) stress, and μ' is the apparent friction, which takes into account reductions in friction due to pore pressure changes. Having no information on the absolute stress field, this calculation only considers how the stress field has evolved since a particular time.

We concentrated our Coulomb stress calculations on three of the most seismically active regions in Alaska: the megathrust along the plate interface, the Fairweather and Queen-Charlotte Fault system, and the central Denali fault. Figure 6 shows calculated Coulomb stress changes resolved on the megathrust from 1949 (time of first earthquake considered) to 2002 (just before the Denali earthquake) due to the three components of the earthquake cycle, individually and combined. The motion of the Pacific plate is shown to load (warm colors) the locked megathrust towards failure (Figure 6a). Coseismic slip then relieves stress on the two primary slip patches (blue regions) associated with the 1964 earthquake (Figure 6b). Slip on these patches also causes an increase in Coulomb stress in surrounding fault regions. Coulomb stress increase between the slip patches was inferred to potentially have induced on-going afterslip, as discussed previously. Viscoelastic relaxation within the lower crust and mantle wedge serves to partially reload the slip patches as shown in Figure 6c. The cumulative stress change since 1949 suggests that the 1964 rupture surface has not yet recovered the stress drop associated with that earthquake, though stress has increased significantly in surrounding regions (Figure 6d). The region along the megathrust to the west, between the 1964 rupture surface and the Shumagin gap (blue region in western part of Figure 6d) and to the east near Yakataga, is the next likely region for large earthquakes.

Figure 7 shows calculated Coulomb stress changes resolved on the Fairweather and Queen-Charlotte transform boundary from 1949 to 2002 due to the three components of the earthquake cycle and combined. Interseismic motion of the Pacific plate is shown to load the locked boundary towards failure (Figure 7a), while coseismic slip associated with the 1949, 1958, and 1972 relieves this stress along the entire length of the fault in this region (Figure 7b). Viscoelastic relaxation within the lower crust and mantle then serves to partially reload the rupture surface and unload the region to the east (Figure 7c). Note how both coseismic and postseismic Coulomb stress changes along the Fairweather Fault serve to unload the southern continuation of the eastern Denali Fault i.e., the Duke River-Dalton-Chatham faults, perhaps explaining why they are no longer active [Lahr and Plafker, 1980]. The cumulative stress change calculation suggests that the plate interface between Queen Charlotte and Vancouver Islands (southeastern corner of Figure 7d) has accumulated significant stress since 1949.

Figure 8 shows calculated Coulomb stress changes resolved on the Denali Fault from 1949 to 2002 due to the three components of the earthquake cycle. Interseismic deformation is shown to increase Coulomb stress all the way from the plate interface to the Denali Fault (Figure 8a), supporting the idea that the Denali fault is a result of partitioning of strain associated with oblique convergence of the Pacific plate. Coseismic slip associated with the 1964 earthquake does not significantly influence Coulomb stress on the Denali fault (Figure 8b), but ~4 decades of viscoelastic relaxation leads to an increase in Coulomb stresses along a major part of the fault that subsequently ruptured in 2002 (Figure 8c). This demonstrates how postseismic relaxation

can influence faults hundreds of kilometers away from great earthquakes. The total stress change resolved on the Denali Fault shows it to be significantly loaded in the past 50 years leading up to the 2002 rupture (Figure 8d). This increase in stress allowed the rupture, which originated in the west to propagate eastward with relative ease.

5. Conclusions

5.1 Posstseismic Study

We developed 2-D and 3-D numerical models to calculate how interseismic deformation due to relative plate motions, large earthquakes, and postseismic processes contribute to the contemporary velocity field and the evolution of the stress in the Alaskan crust. 2-D models show that interseismic deformation is best simulated using a modified backslip model. Using the modified backslip approach, a 3-D model showed that northerly-directed velocities could be explained by subduction of the Pacific plate with a megathrust locked to a depth of 30 km. This model leads to interseismic velocities that drop off dramatically above the location of the maximum locking depth of the megathrust below. Flat subduction beneath the Yakutat microplate increases the width of the locking zone, pushing the region where interseismic velocities drop off further inland. While northerly directed surface velocities within Alaska are well explained by the convergence of the Pacific plate, southerly directed velocities in the vicinity of the 1964 rupture zone to well north of the Denali fault are well explained by viscoelastic relaxation of the lower crust and upper mantle (order 10^{19} Pa s) following the 1964 Alaska earthquake. This transient model cannot, however, explain observed southerly velocities very close to the rupture zone in a region that lies between the two primary slip patches of the 1964 earthquake. Afterslip within this region combined with postseismic relaxation and interseismic deformation explains observed surface velocities within this region and throughout most of Alaska.

We used the 3-D model to calculate the evolution of stress in the Alaskan crust associated with interseismic deformation, coseismic slip associated with the 1964 megathrust earthquake and three events along the Fairweather and Queen-Charlotte faults (in 1949, 1958 and 1972), and viscoelastic relaxation associated with these events. Interseismic model results suggested that contemporary stressing rates, both compressional and shear, are greatest within a band of crust that overlies the down-dip edge of the locked portion of the megathrust. Because of shallow subduction beneath the Yakutat microplate, this increases the inland reach of high compression and shear stresses. Interseismic deformation was shown to load the megathrust and the transform plate boundary to the east. Interseismic deformation was also shown to load the Denali Fault, suggesting that this fault acts to partition strain associated with oblique subduction. Coseismic stresses were shown to relieve interseismic stresses along the megathrust, while loading the surrounding regions. Coseismic stresses along the transform boundary serve to relieve stresses on the fault as well as regions to the east. Postseismic relaxation was shown to reverse the trend of coseismic stresses on the megathrust and surrounding regions, while on the transform fault postseismic relaxation works to reload the fault but relieves stress to the east. Of particular interest is the result that postseismic relaxation following the 1964 earthquake worked to load the rupture surface of the 2002 Denali earthquake several hundred kilometers inland.

5.2 Totschunda-Fairweather Fault

The neotectonic framework of southeastern Alaska is still only partly understood due to its remote setting and steep, highly glaciated topography. In this type of setting, thin-shell finite-

element models provide a useful tool for discriminating between contrasting fault geometries and lithospheric strength profiles. To evaluate the organization of contemporary faulting in southern Alaska, we tested our models against known geologic slip rates at a number of locations. The best-fit model uses a relatively weak lower crust and upper mantle rheology and requires a continuum of strikeslip deformation between the Totschunda and Fairweather faults located in the St. Elias Mountains. We refer to this inferred zone of deformation as the Fairweather–Totschunda connecting fault; this fault slips at a predicted rate of 8 mm/a in our best-fit model. As noted by previous authors, minimal offset (~0.5 km) of units require the Fairweather–Totschunda connecting fault to be a recently established strike-slipboundary. Results suggest that the Fairweather, Totschunda, and Fairweather–Totschunda connecting faults, along with central segments of the Denali fault, are the principle means of strain accommodation in southern Alaska. The eastern Denali fault, in contrast, is calculated to have a comparatively low rate of slip (<3 mm/a) and thus may no longer play a significant role in strain accommodation. The model results along with available geologic data from faults in southeastern Alaska and the western Yukon Territory suggest that the strike-slip deformation front in southeastern Alaska may have stepped progressively southwestward to maintain a regional fault orientation conducive for transport of crustal material through the syntaxis. The best-fit model also suggests that the Transition fault at the trailing edge of the Yakutat microplate slips at a rate of 23 mm/a and, therefore, that the Yakutat microplate and the Pacific plate are not moving as a single entity. Slip rates on the Transition fault must diminish to the east, as the model indicates that shear strain accommodated by the Fairweather fault is not being bled off by the Transition fault.

References

1. Aagaard B., Williams C. and Knepley M., PyLith: A finite-element code for modeling quasi-static and dynamic crustal deformation, EOS Trans. AGU, 89(53), Fall Meet. Suppl., Abstract T41A-1925, 2008.
2. Aagaard, B., Kientz S., Knepley M., Strand L. and Williams C., *PyLith User Manual*, v1.4, Pasadena, CA: Computational Infrastructure of Geodynamics, 2009. URL: geodynamics.org/cig/software/short/pylith/pylith_book-1.4.pdf
3. Cohen S.C. and Freymueller J.T., Crustal Deformation in Southcentral Alaska: The 1964 Prince William Sound Earthquake Subduction Zone, Adv. Geophys., 47, p.1-63, 2004.
4. DeMets C., Gordon R.G., Argus D.F., and Stein S., Effect of recent revisions to the geomagnetic reversal timescale on estimates of current plate motions, Geophys. Res. Lett., 21, p.2191-2194, 1994.
5. Eberhart-Phillips D. et al., The 2002 Denali Fault Earthquake, Alaska: A Large Magnitude, Slip-Partitioned Event, Science, 300, p.1113-1118, 2003.
6. Eberhart-Phillips D., Christensen D.H., Brocher T.M., Hansen R., Ruppert N.A., Haeussler P.J., and Abers G.A., Imaging the transition from Aleutian subduction to Yakutat collision in central Alaska, with local earthquakes and active source data, J. Geophys. Res., 111, B11303, doi:10.1029/2005JB004240, 2006.
7. Freed A.M., Burgmann R., Calais E., Freymueller J.T. and Hreinsdottir S., Implications of deformation following the 2002 Denali, Alaska earthquake for postseismic relaxation processes and lithospheric rheology, J. Geophys. Res., 111, B01401, doi:10.1029/2005JB003894, 2006a.
8. Freed A. M., Earthquake triggering by static, dynamic, and postseismic stress transfer, *An. Rev. Earth Planet. Sci.,* 33, p.335-367, 2005.
9. Freed A.M., Burgmann R., Calais E. and Freymueller J., Stress-dependent power-law flow in the upper mantle following the 2002 Denali, Alaska, earthquake, Earth Planet. Sci. Lett., 252, p.481-489, 2006b.
10. Freymueller J.T., Woodard H., Cohen S.C., Cross R., Elliott J., Larsen C.F., Hreinsdottir S. and Zweck C., Active Deformation Processes in Alaska, Based on 15 Years of GPS Measurements, in Active Tectonics and Seismic Potential of Alaska, Geophysical Monograph Series, 179, 2008.
11. Hetland E.A. and Hager B.H., Interseismic strain accumulation: Spin-up, cycle invariance, and irregular rupture sequences, Geochem. Geophys. and Geosyst., 7, Q05004, doi:10.1029/2005GC001087, 2006.
12. Jaeger J. and Cook N., Fundamentals of Rock Mechanics, 3rd ed., Chapman and Hall, London, 1979.
13. Johnson M., Satake K., Holdahl R. and Sauber J., The 1964 Prince William Sound earthquake: Joint inversion of tsunami and geodetic data, J. Geophys. Res., 101, p.523-532, 1996.
14. Kanamori H., The energy release of great earthquakes, J. Geophys. Res. 82, p.2981-2987, 1977.

15. King G.C.P., Stein R.S. and Lin J., 1994. Static stress changes and triggering of earthquakes, Bull. Seism. Soc. Am., 84, p.935-953., 1994.

16. Lahr J.C. and Plafker G., Holocene Pacific–North American plate interaction in southern Alaska: Implications for the Yakataga seismic gap, Geology, 8, p.483-486, 1980.

17. Larsen C.F., Motyka R.J., Freymueller J.T., Echelmeyer K.A. and Ivins E.R., Rapid uplift of southern Alaska caused by recent ice loss, Geophys. J. Int., 158, p.1118-1133, 2004.

18. Larsen C.F., Motyka R.J., Freymueller J.T., Echelmeyer K.A. and Ivins E.R., Rapid viscoelastic uplift in southeast Alaska caused by post-Little Ice Age glacial retreat, Earth Planet. Sci. Lett., 237, p.548-560, 2005.

19. Nishenko S.P. and Jacob K.H., Seismic potential of the Queen Charlotte-Alaska-Aleutian seismic zone, J. Geophys. Res., 95, p.2511-2532, 1990.

20. Parker J., Lyzenga G., Norton C. et al., Geophysical finite-element simulation tool (GeoFEST): Algorithms and validation for quasistatic regional faulted crust problems, Pure Appl. Geophys., 165, p.497-521, 2008.

21. Pollitz F.F., Transient rheology of the upper mantle beneath central Alaska inferred from the crustal velocity field following the 2002 Denali earthquake, J. Geophys. Res., 110, B08407, doi:10.1029/2005JB003672, 2005.

22. Sauber J., Plafker G., Molnia B. and Bryant M., Crustal deformation associated with glacial fluctuations in the eastern Chugach Mountains, Alaska, J. Geophys. Res., 105, 8055-8077, 2000.

23. Stein R.S. and Lisowski M., The 1979 Homestead Valley earthquake sequence, California: control of aftershocks and postseismic deformation, J. Geophys. Res., 88, p.6477-6490, 1983.

24. Suito H. and Freymueller J.T., A viscoelastic and afterslip postseismic deformation model for the 1964 Alaska earthquake, J. Geophys. Res., doi:10.1029/2008JB005954, 2009.

25. Veenstra E., Christensen D.H., Abers G.A. and Ferris A., Crustal thickness variation in south-central Alaska, Geology, 34, p.781-784, 2006.

26. Zhao S. and Takemoto S., Deformation and stress change associated with plate interaction at subduction zones: a kinematic modeling, Geophys. J. Int., 142, p.300-318, 2000

27. Zweck C., Freymueller J.T. and Cohen S.C., Elastic dislocation modeling of the postseismic response to the 1964 Alaska Earthquake, J. Geophys. Res., 2001JB000409, 2002.

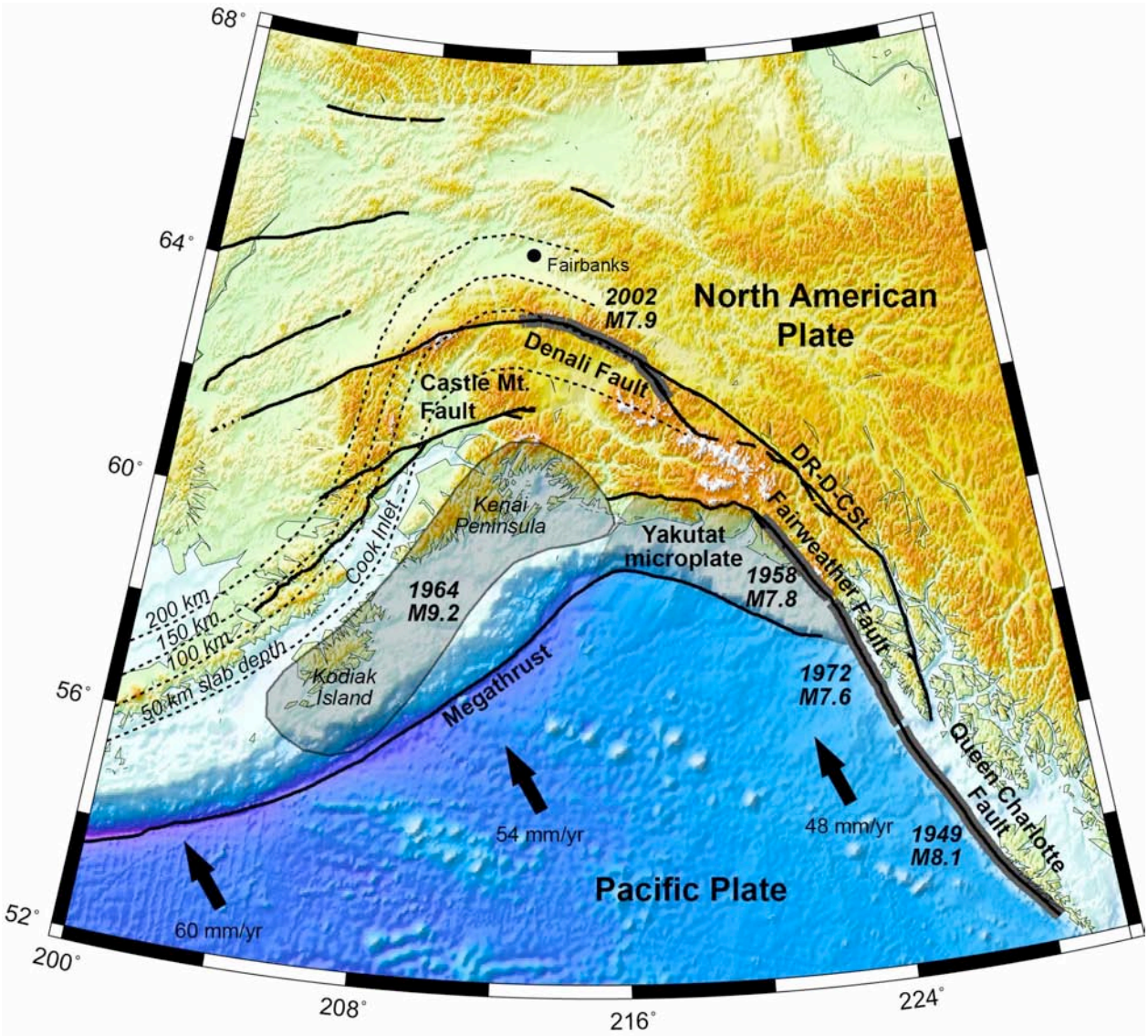

Figure 1. Map showing tectonic setting of Southern Alaska and surrounding region. Pacific slab depth contours shown as grey dashed lines. The rupture surfaces of the five earthquakes considered in this study are shown as grey lines/regions (see Table 1 for references). The Yakutat microplate is also shown in grey. Pacific plate velocities are based after DeMets et al. [1994].

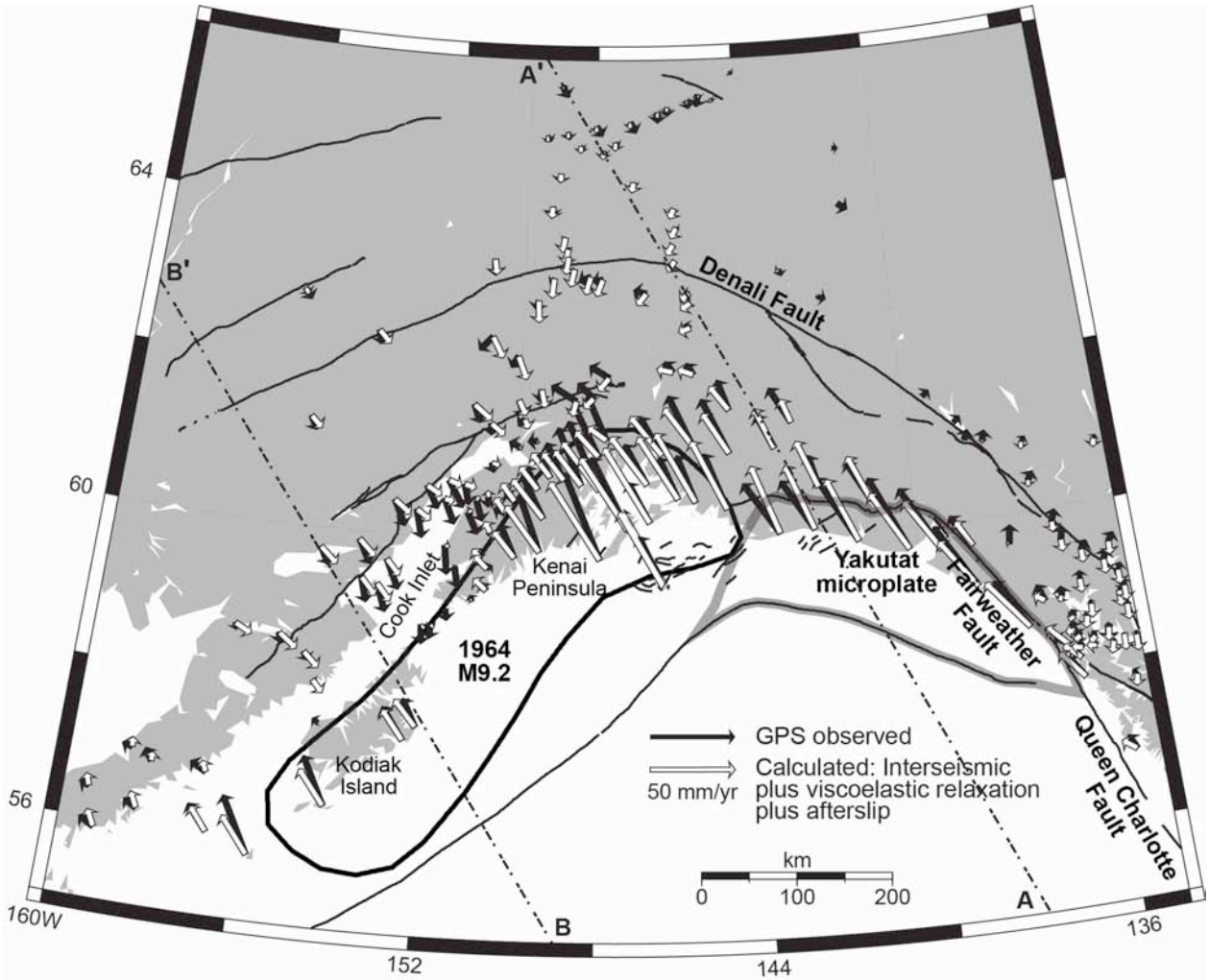

Figure 2. Average horizontal velocities in Alaska (w.r.t. stable North America) as observed by GPS from 1997 to 2002 and those calculated by a combined interseismic, viscoelastic relaxation, and afterslip model (see text). Cross-section A-A' is where a 2-D model is used to explore interseismic deformation across the Yakutat microplate. Cross-section B-B' is where a 2-D model is used to explore interseismic and postseismic deformation across the 1964 Alaska earthquake rupture zone. GPS velocities are from Freymueller et al. [2008]. For clarity, only a subset of the GPS velocities are shown.

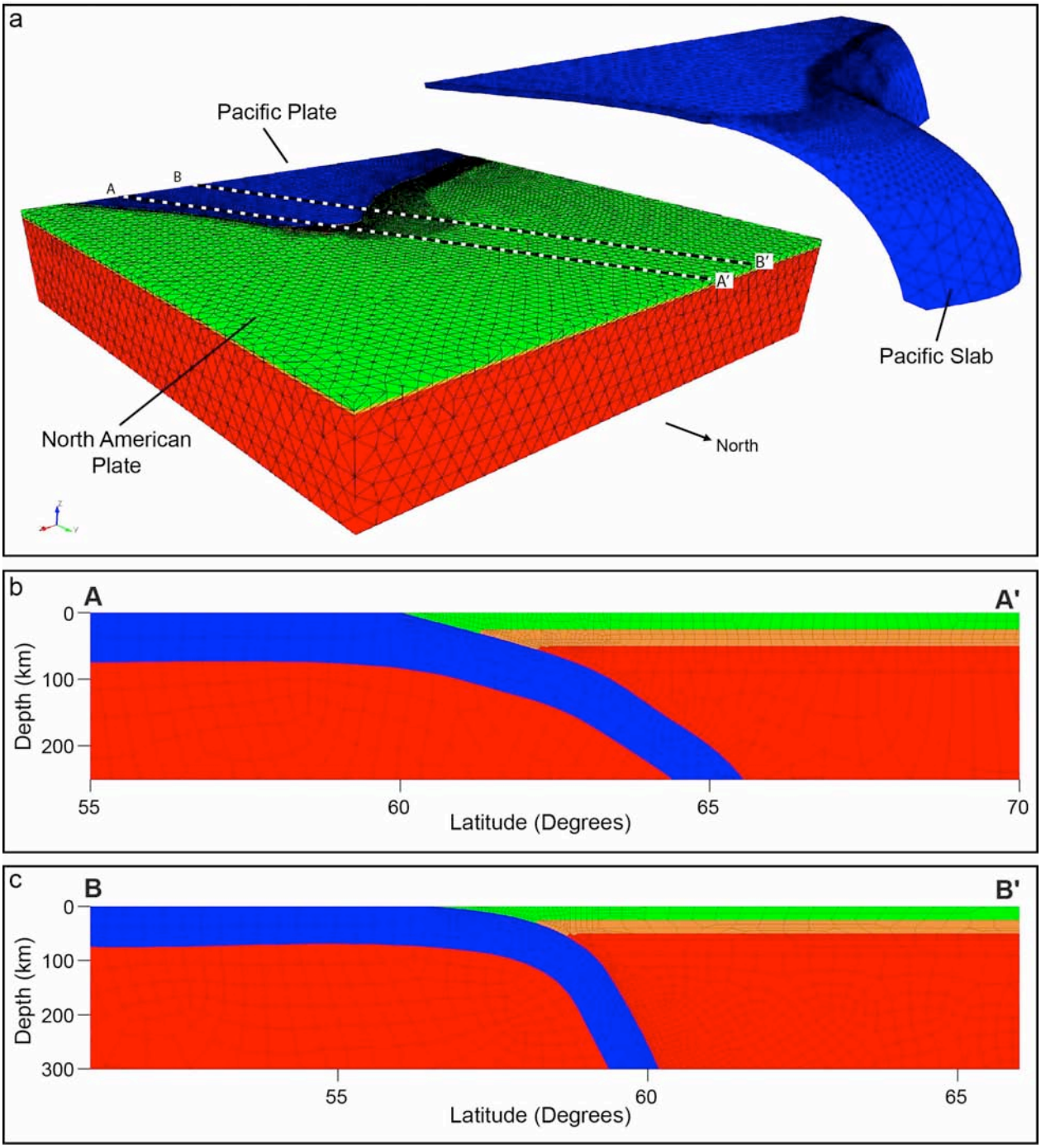

Figure 3. Finite element meshes used in this study. (a) Full 3-D model with slab geometry shown in inset. (b) Part of the 2-D mesh used for interseismic calculations through cross-section A-A' in Figure 2. (c) Part of 2-D mesh used for interseismic and postseismic calculations through cross-section B-B' in Figure 2. The actual meshes for (b) and (c) extends a few hundred kilometers on all three sides. The continental (in green) and oceanic crust (in blue) have a shear modulus of 39 GPa and 52 GPa respectively. The shear modulus for the mantle (red) is assumed to be 69 GPa. Poisson's ratio for all materials is assumed to be 0.25.

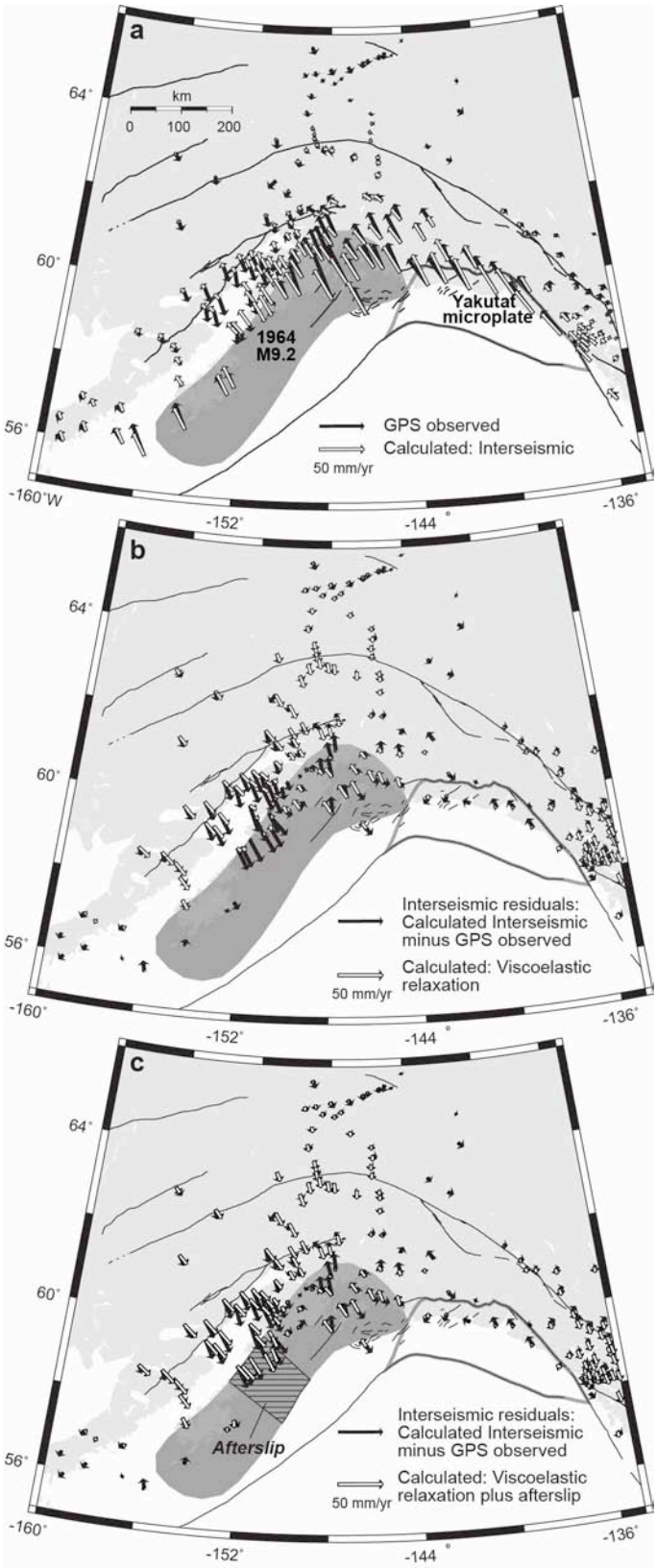

Figure 4. (a) Comparison of GPS observed versus calculated horizontal surface velocities based on a model of interseismic deformation using a modified backslip model. (b) Comparison of residual velocities (GPS observed minus interseismic deformation) versus calculated velocities based on viscoelastic relaxation. (c) Comparison of residual versus calculated velocities based on viscoelastic relaxation plus afterslip. See text for model details.

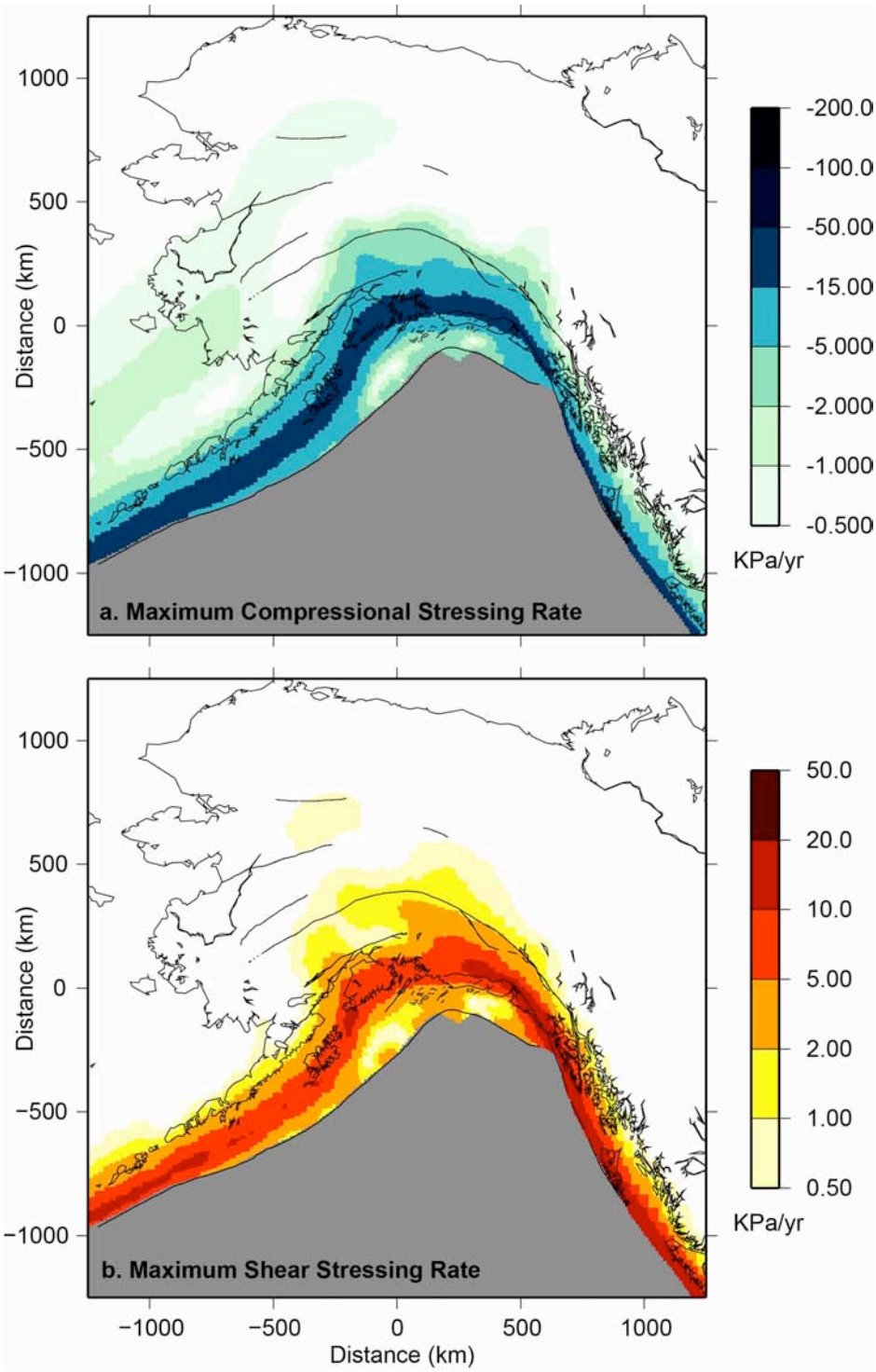

Figure 5. (a) Maximum compressive and (b) maximum shear stressing rates at the surface of the North American crust associated with the interseismic deformation.

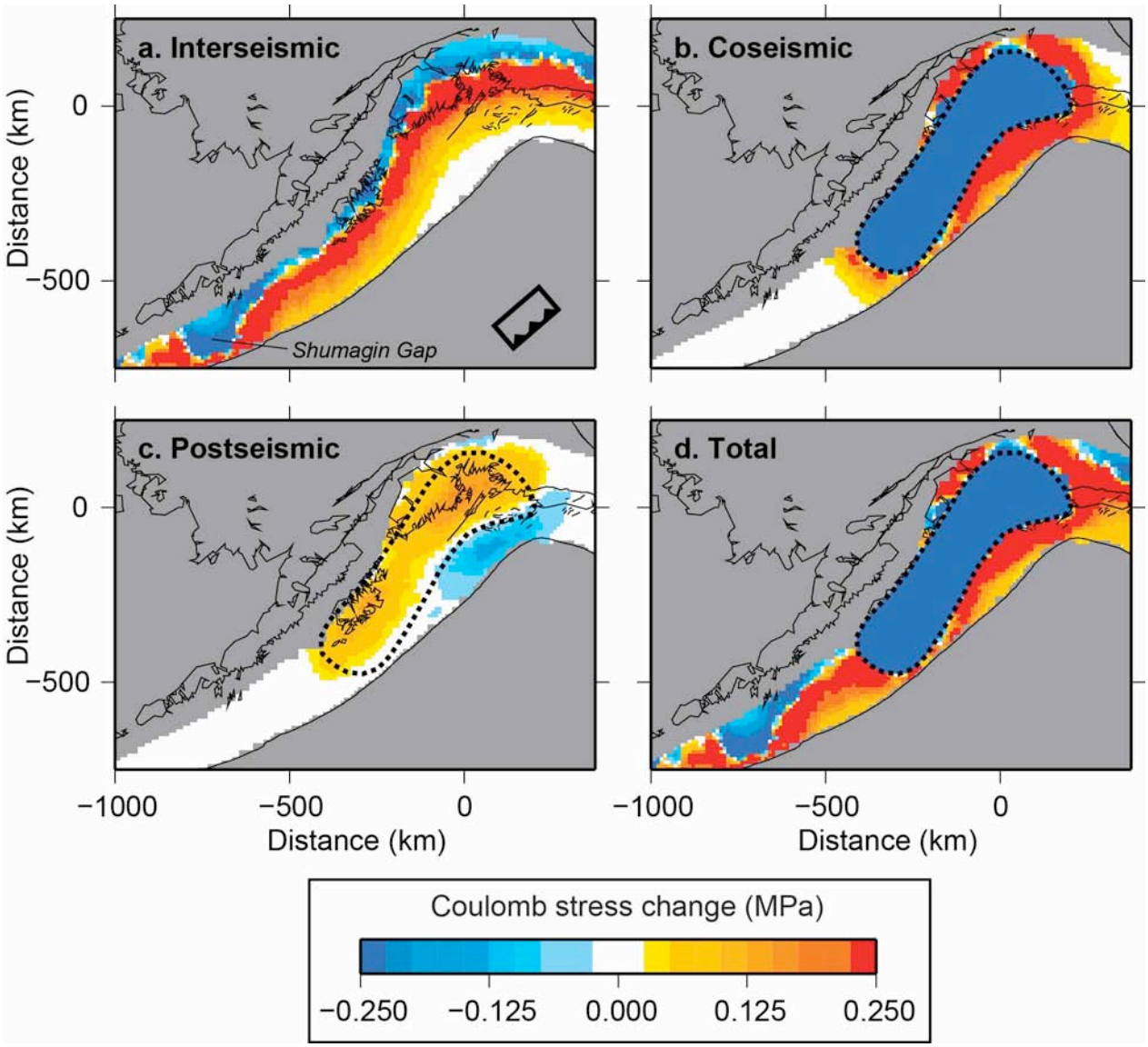

Figure 6. Coulomb stress change resolved on the Pacific megathrust from 1949 to 2002 due to (a) interseismic deformation, (b) coseismic slip, (c) postseismic viscoelastic relaxation, and (d) interseismic plus coseismic slip plus viscoelastic relaxation. The Shumagin gap where the locked depth is inferred to be only ~5 km deep is noted. The edge of the 1964 rupture surface is shown as a dashed line in (b-d). Coulomb stress change is calculated on thrust faults striking N47°E with a dip angle of 10 degrees, based on an apparent friction coefficient of 0.1. Stresses on the megathrust are shown to a depth of 35 km, beyond which the dip angle is too steep for the calculated Coulomb stress component.

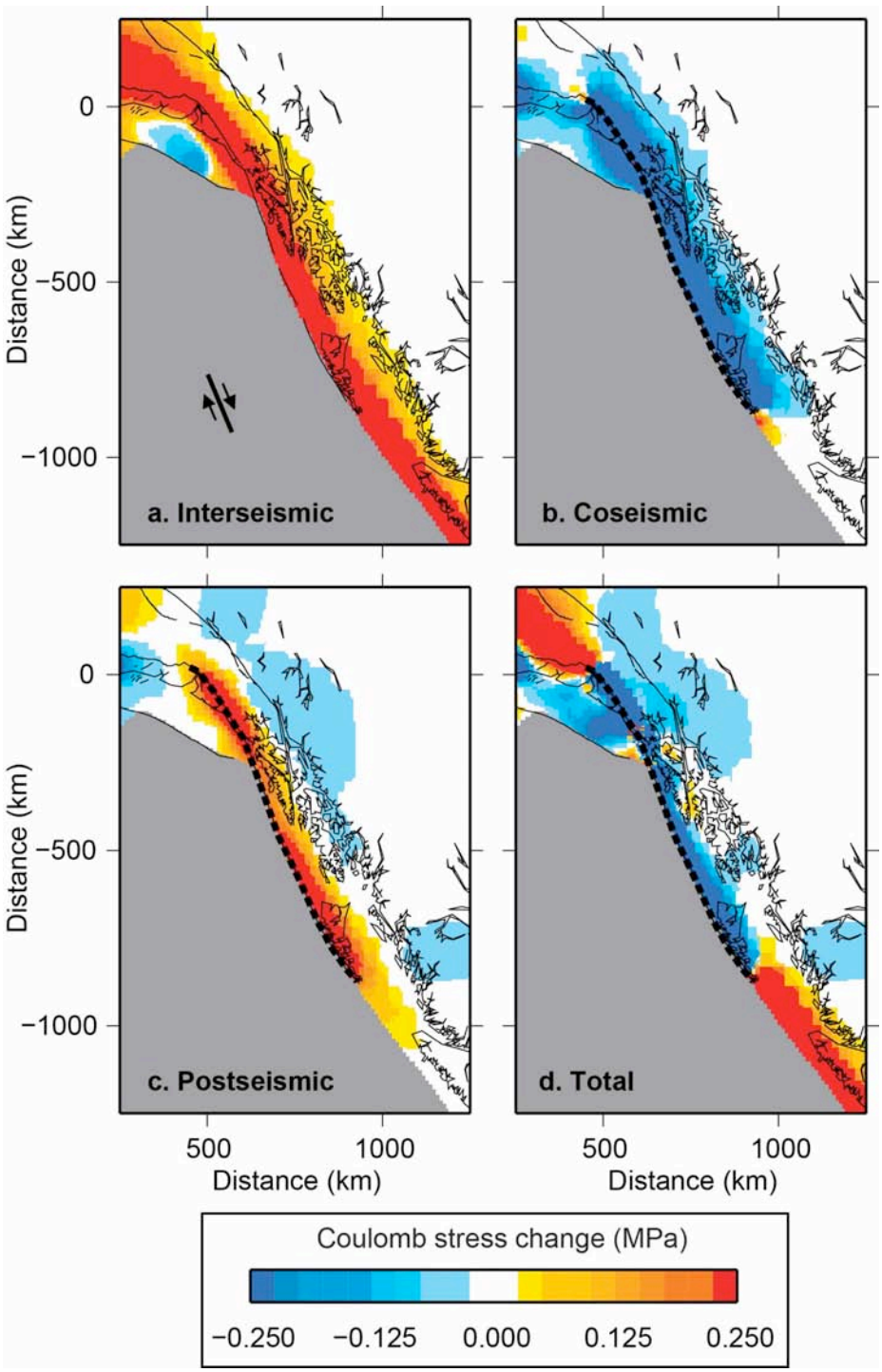

Figure 7. Coulomb stress change resolved on the Fairweather and Queen-Charlotte faults from 1949 to 2002 due to (a) interseismic deformation, (b) coseismic slip, (c) postseismic viscoelastic relaxation, and (d) interseismic plus coseismic slip plus viscoelastic relaxation. The extent of the rupture surface of the 1949, 1958, and 1972 events on this transform boundary is shown as a black dashed line in (b-d). Coulomb stress change is calculated on vertical right lateral strike slip faults striking N70°E, based on an apparent friction coefficient of 0.1. Stresses are not recovered for the Pacific plate, which is blacked out in the figures.

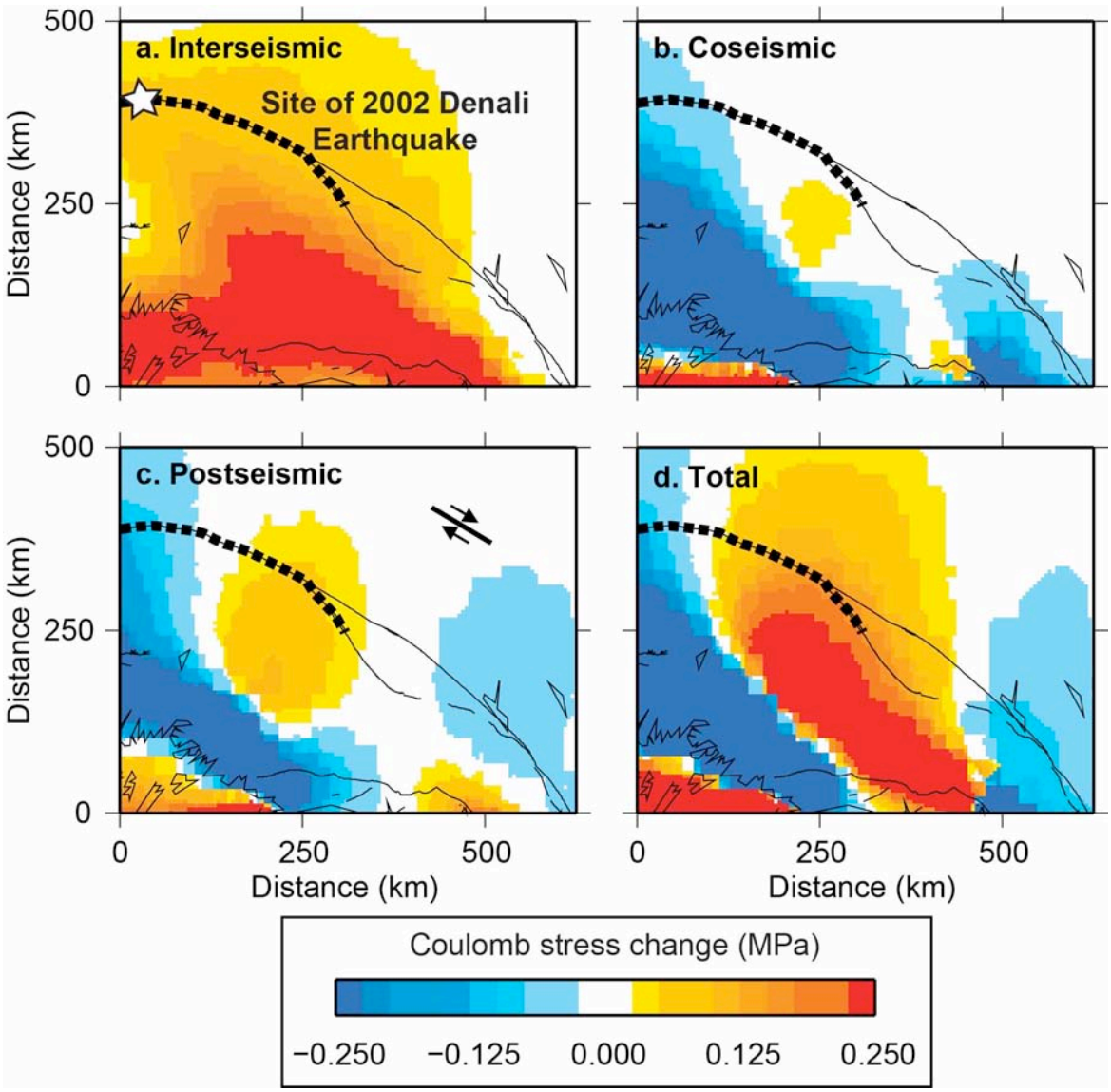

Figure 8. Coulomb stress change resolved on the central Denali Fault from 1949 to 2002 due to (a) interseismic deformation, (b) coseismic slip, (c) postseismic viscoelastic relaxation, and (d) interseismic plus coseismic slip plus viscoelastic relaxation. The rupture surface of the 2002 Denali earthquake (though not ruptured for this calculation) is shown as a bold dashed line. Coulomb stress change is calculated on vertical right lateral strike slip faults striking N30°E, based on an apparent friction coefficient of 0.1.